Molecular characterization of gustatory second-order neurons reveals integrative mechanisms of gustatory and metabolic information

Rubén Mollá-Albaladejo[1], Manuel Jiménez-Caballero[1] and Juan A. Sánchez-Alcañiz[1]*

[1]Instituto de Neurociencias, CSIC-UMH, San Juan de Alicante, Spain
*Corresponding author
email: juan.sanchez@umh.es

Abstract

Animals must balance the urgent need to find food during starvation with the critical necessity to avoid toxic substances to ensure their survival. In *Drosophila*, specialized Gustatory Receptors (GRs) expressed in Gustatory Receptor Neurons (GRNs) are critical for distinguishing between nutritious and potentially toxic food. GRNs project their axons from taste organs to the Subesophageal Zone (SEZ) in the Central Brain (CB) of *Drosophila*, where gustatory information is processed. Although the roles of GRs and GRNs are well-documented, the processing of gustatory information in the SEZ remains unclear. To better understand gustatory sensory processing and feeding decision-making, we molecularly characterized the first layer of gustatory interneurons, referred to as Gustatory Second-Order Neurons (G2Ns), which receive direct input from GRNs. Using trans-synaptic tracing with *trans*-Tango, cell sorting, and bulk RNAseq under fed and starved conditions, we discovered that G2Ns vary based on gustatory input and that their molecular profile changes with the fly's metabolic state. Further data analysis has revealed that a pair of neurons in the SEZ, expressing the neuropeptide Leucokinin (SELK neurons), receive simultaneous input from GRNs sensing bitter (potentially toxic) and sweet (nutritious) information. Additionally, these neurons also receive inputs regarding the starvation levels of the fly. These results highlight a novel mechanism of feeding regulation and metabolic integration.

Introduction

Animals face constant dangers in their environment that they must avoid to survive, being starvation and poisoning two critical threats. To prevent death by starvation, animals must continually seek food, even if it means risking consumption of potentially harmful substances[1–3]. Therefore, accepting or rejecting food potentially poisonous will depend on the general nutritious content and toxicity of the meal, together with the starvation level of the animal. Similar to other animals, *Drosophila melanogaster* can discern different taste qualities (sweet,

bitter, salty, sour, umami or carbonation) through various populations of Gustatory Receptor Neurons (GRNs) tuned to each of these qualities[4]. GRNs are distributed across the *Drosophila*'s body including the proboscis, legs, wing margins, and the ovipositor organ, expressing a combination of receptors for detecting various food compounds[5]. There are four major families of receptors involved in gustatory perception: Gustatory Receptors (GRs), Ionotropic Receptors (IRs), Transient Receptor Proteins (TRPs), and pickpocket (ppk) channels[6]. Specific GRNs are associated with particular valences, such as sweet or bitter tastes. For instance, Gr64f is a receptor for sugar detection promoting feeding behavior[7,8], while Gr66a is present in GRNs that detect bitter compounds leading to feeding rejection[9,10].

GRNs project their axons to the Subesophageal Zone (SEZ), the main brain region in flies for integrating and processing gustatory information. Unlike the olfactory system, where olfactory sensory neurons expressing the same receptors converge in the same glomeruli to synapse with projection neurons, the gustatory system lacks such anatomical subdivisions[5,11]. However, neurons expressing receptors that respond to sweet compounds and elicit attractive behaviors converge in specific SEZ regions without overlapping neurons detecting bitter compounds and inducing feeding rejection[10,12].

The development of extensive collections of Gal4 lines[13], split-Gal4 collections[14], and databases for searchable neurons[15], has facilitated the identification of gustatory interneurons in the SEZ involved in feeding behavior. Those databases have been used to design experimental procedures that has help to the identification of some gustatory interneurons involved in integrating gustatory information and inducing feeding[1,16–22]. These studies have identified command neurons critical for feeding behavior, some directly receiving input from GRNs, such as certain GABAergic neurons[1], while others, like the Feeding neuron (Fdg), act as a hub to control food acceptance without being connected directly to any GRN[16]. Despite these advances, the role of gustatory interneurons in integrating gustatory information and the metabolic state of the fly remains largely unexplored. The recent development of the *Drosophila* brain connectome through electron microscopy is advancing our understanding of SEZ connectivity and the complex interactions among GRNs[23,24].

We have aimed to elucidate the integration of gustatory information and the metabolic state, by analyzing the first layer of interneurons that collect gustatory information, Gustatory Second-Order Neurons (G2Ns)[23]. We have decided to focus on understanding how flies integrate gustatory information that codes for opposing behaviors: sweet tastants elicit feeding whereas bitter compounds induce food rejection[11]. We have followed a molecular approach to identify G2Ns. First, we employed the *trans*-Tango genetic tool[25], which labels postsynaptic neurons connected to specific presynaptic neurons. Later, using Fluorescent Activated Cell Sorting (FACS) of labeled G2Ns and bulk RNA sequencing (RNAseq), we characterized the molecular profiles of postsynaptic neurons connected to sweet and bitter GRNs in fed and

starved conditions for the first time. These analyses show that G2Ns receive input from molecularly distinct GRNs, and their transcriptional profiles change upon starvation, presumably to adapt to the new metabolic state. Using molecular and connectomic techniques, we further demonstrate that the two *Leucokinin*-expressing neurons in the SEZ (SELK neurons) are G2Ns that simultaneously receive sweet and bitter GRN input. Behavioral experiments revealed that Leucokinin neurons integrate information regarding the metabolic state of the fly and are involved in the processing of bitter and sweet information that impacts the initiation of feeding behavior.

Results

Molecular characterization of gustatory second-order neurons

We employed the trans-synaptic tracing method *trans*-Tango[25], to label G2Ns synaptically connected to sweet and bitter GRNs. To label G2Ns receiving sweet information, we used the *Gr64f-Gal4* transgene[7,10], and for G2Ns receiving bitter information, we used the *Gr66a-Gal4* transgene[10,26]. These Gal4 transgenes enabled us to label multiple G2Ns of interest (**Sup. Figure 1.1A and B**). The number of postsynaptic G2Ns differed between the GRNs, indicating differences in information processing for different tastants (**Sup. Figure 1.1C and D**). Since satiety and hunger significantly influence behavior, modifying olfactory behavior[27], memory formation[28] and food consumption[2,29], we extended our analysis to characterize molecularly G2Ns receiving different gustatory inputs in two metabolic states: fed and 24-hour starved flies. Given that all G2Ns are fluorescently labeled with mtdTomato, we used FACS to separate and collect the cells for bitter and sweet G2N populations ($Gr66a^{G2Ns}$ and $Gr64f^{G2Ns}$, respectively) in the two metabolic conditions (see Materials and Methods for a detailed description of the sorting procedure and sample number in **Table 1**). We then performed bulk RNAseq for each condition (**Figure 1A**).

The data's Principal Component Analysis (PCA) revealed that the transcriptomic profiles of the two G2N populations are different and that the metabolic state (fed vs. starved) significantly influences gene expression without affecting the separation among the populations in the PC space (**Figure 1B**). These findings suggest that the first layer of neurons collecting sensory information is already modulated by the fly's metabolic state, potentially impacting subsequent information processing.

We further analyzed the changes in gene expression between fed and starved conditions across the two G2N populations. Many genes exhibited differential expression in starved flies compared to fed flies (**Figure 1C**). Gene Ontology (GO) analysis indicated that several genes were involved in nervous system development and synapse organization,

suggesting the importance of synapse remodeling during starvation adaptation. Additionally, GO terms related to the response to sensory stimuli and stress response were identified, implying that starvation induces molecular signatures of stress in flies. Finally, some genes associated with signaling pathways indicated that neurotransmitter and neuropeptide signaling processes might be altered during starvation, leading to specific adaptations in the neuronal circuits involving G2Ns (**Sup. Figure 1.2**).

Characterization of neurotransmitter and neuropeptide expression

Next, we focused on the expression of neurotransmitters, neuropeptides, and their respective receptors as they are known to modulate feeding among many other behaviors[30]. For example, the CCHamide 1 receptor regulates starvation-induced olfactory modulation[31]; NPF (Neuropeptide F) modulates taste perception in starved flies by increasing sensitivity to sugar and decreasing sensitivity to bitter by promoting GABAergic inhibition onto bitter GRNs[2]; starvation enhances behavioral sugar-sensitivity via increased dopamine release onto sweet GRNs, indirectly decreasing sensitivity to bitter tastants[32]; and octopamine signaling affects bitter signaling in starved flies[3].

Our RNAseq data revealed that the most prominent neurotransmitter receptor expressed in all G2Ns was *nAChRbeta1* (nicotinic Acetylcholine Receptor Beta 1) (**Figure 2A**). This is consistent with previous findings showing that GRNs are mostly cholinergic[33]. Other acetylcholine and neurotransmitter receptors were also expressed in G2Ns. This indicates that while G2Ns receive significant input from GRNs, they also integrate information from a complex network of other neurons using different neurotransmitters. We found no variation in expression levels for any neurotransmitter receptors when comparing fed and starved conditions. Regarding neurotransmitter expression, *Gad1* (Glutamic acid decarboxylase 1) and *Ddc* (Dopa decarboxylase), two essential enzymes involved in the synthesis of GABA and dopamine, respectively, were highly expressed in the two G2N populations for both metabolic states (**Figure 2B**). Other enzymes involved in the GABA pathway, like *VGAT* (vesicular GABA transporter) or *GABAT* (γ-aminobutyric acid transaminase), were also expressed but at lower levels than *Gad1*. Similarly, other enzymes or transporters related to other neurotransmitters, like glutamate (Glu) or serotonin (5-HT), were present but at lower levels.

Regarding neuropeptide receptors, we found many receptors expressed in all G2Ns populations with varying expression levels (**Figure 2C**). For instance, the *EcR* (Ecdyson Receptor) showed expression in all three populations with a slight decrease under starvation, indicating a possible role in adapting to food deprivation. Additionally, *sNPF-R* (short Neuropeptide F Receptor) was highly expressed with similar expression patterns as its ligand

sNPF (short Neuropeptide F), highlighting the importance of sNPF and its signaling pathway in regulating starvation and feeding[34–36].

Neuropeptides showed variable expression patterns between populations and conditions (**Figure 2D**). For example, *sNPF* was highly expressed in all G2Ns, particularly in the Gr66a^{G2N} population, without changes associated with the metabolic state. sNPF production, which is related to circulating sucrose levels, impacts food intake by integrating sweet and bitter information in food-deprived flies[2]. This highlights the role of sNPF and its receptor (sNPF-R) in regulating the feeding behavior according to the metabolic state, as it is secreted in the midgut and by neurosecretory cells in the brain. Dh31 (Diuretic hormone 31) and Dh44 (Diuretic hormone 44), which are involved in desiccation tolerance and starvation adaptation[37], also showed notable expression in both G2N populations under starved and fed conditions. Nplp1 (Neuropeptide-like precursor 1), which is associated with synaptic organization in the nervous system and water balance[30], was also expressed in both G2Ns. Among all neuropeptides, however, Leucokinin (Lk) displayed the most striking expression change. Though *Lk* has no (or very low) expression in the Gr64f^{G2N} population under fed and starved conditions, and no (or very low) expression in the Gr66a^{G2N} under fed conditions, *Lk* showed significantly elevated expression in the Gr66a^{G2N} population under starved conditions. This expression pattern specific to Gr66a^{G2Ns} suggests that Lk may play a role in processing bitter information under starvation. We decided to explore this neuropeptide further to understand its role in integrating feeding behavior and the metabolic state of the flies.

Leucokinin expression is upregulated SELK neurons in the starved condition

Leucokinin is a neuropeptide with multiple roles in various physiological and behavioral processes[38]. Three different Lk neuron groups exist in the adult *Drosophila* Central Nervous System (CNS). There are approximately 20 Lk neurons in the Ventral Nerve Cord (ABLKs), while in the CB, there are four Lk neurons, two located in the Lateral Horn (LHLK) and another two located in the SEZ (SELK)[39,40]. ABLKs use Lk as a hormonal signal targeting peripheral tissues, including renal tubules, to regulate water and ion homeostasis in response to desiccation, starvation, and ion stress, as Lk regulates fluid secretion in the Malpighian (renal) tubules[40]. LHLK neurons are part of the output circuitry of the circadian clock, regulating locomotor activity and sleep suppression induced by starvation[41–44]. Functional imaging revealed that LHLK neurons, not SELK neurons, were required to suppress sleeping during starvation[44]. It has been suggested that SELK neurons may regulate feeding as possible synaptic partners to the premotor feeding program. However, it is still not clear the role of SELK neurons in feeding behavior[38,40].

Due to the dissection method used for our RNAseq experiment (**Figure 1A**), we primarily captured SELK neurons rather than LHLK neurons. To confirm that starvation induces changes in *Lk* gene expression, we performed qPCR on brains from fed and starved *Drosophila*. Given that Lk neurons constitute 4 out of approximately 200.000 neurons in the *Drosophila* brain[45], we enriched our samples by expressing GFP in Lk neurons using the driver *Lk-Gal4*[46] combined with *UAS-mCD8::GFP* transgene and FACS of the GFP^+ cells. We conducted qPCR analysis on the whole CB (including both LHLK and SELK neurons) as well as on the SEZ alone (containing only the 2 SELK neurons) in fed and starved conditions (**Figure 3A and 3B**). Our results showed that starvation increased the expression level of *Lk* mRNA in the CB and also in the SELK neurons, indicating that *Lk* expression is indeed affected by the animal's starvation state (**Figure 3C**). To confirm that the increased mRNA expression translates into higher protein levels, we performed immunohistochemistry using an Lk antibody in fed and 24-hour starved wild-type flies. We quantified the fluorescence in the LHLK and SELK neurons and found that *Lk* expression was elevated under starvation conditions (**Figure 3D-F**) further validating our RNAseq results. Together, these three lines of evidence indicate that SELK neurons increase the expression of the Lk neuropeptide in 24-hour starved flies.

<u>*Leucokinin neurons are gustatory second-order neurons to GRNs*</u>

Our RNAseq data showed that the two SELK neurons receive almost exclusive input from bitter, but not sweet GRNs and that the metabolic state of the fly modulates the expression of *Lk*. To confirm that Lk neurons are indeed postsynaptic partners of bitter GRNs, we used an Lk antibody[39] to test the co-localization of Lk protein with the cells labeled in *GRNs-Gal4 > trans-Tango* flies. These experiments demonstrated that Lk signal colocalizes with trans-Tango in *Gr66a-Gal4 > trans-Tango* flies, confirming our expectations based on the RNAseq data (**Figure 4A**). Unexpectedly, however, we also found co-localization of the Lk antibody signal in *Gr64f-Gal4 > trans-Tango* flies, suggesting that SELK neurons do not receive exclusive input from bitter neurons but also from sweet-sensing neurons expressing the Gr64f receptor (**Figure 4B**).

To validate the synaptic connectivity between $Gr64f^{GRNs}$ and $Gr66a^{GRNs}$ with SELK neurons, we next used the GRASP (GFP Reconstruction Across Synaptic Partners) technique[47]. GRASP can reveal the synaptic connectivity between two neurons, through the expression of half of the GFP protein in each candidate neuron. The reconstruction of the entire GFP protein in the synaptic cleft can be detected by a specific GFP antibody. We expressed half of the GFP (GFP^{11}) protein in the bitter GRNs using *Gr66a-LexA*[48] and sweet GRNs using *Gr64f-LexA*[8] transgenes. The other half of GFP (GFP^{1-10}) protein was expressed

in Lk neurons using the *Lk-Gal4* driver. GRASP results confirmed the synaptic connection between bitter GRNs and sweet GRN with SELK neurons in the SEZ (**Figure 5A and 5C**), further confirming our previous *trans*-Tango result.

The GRASP technique can produce false positives, as a positive signal may result from the proximity of the neurons of interest. We decided to complement those results using active-GRASP[49]. In this modified version, the presynaptic half of GFP (GFP^{1-10}) is fused to synaptobrevin. This fusion allows the GFP to be present in the membrane of the presynaptic neuron within the synaptic cleft when the presynaptic neuron is stimulated. In our experiments, we fed the flies with sucrose to activate sweet GRNs and caffeine to activate bitter GRNs. A positive signal in active-GRASP indicates synaptic connectivity between the candidate neurons and active communication between them. Our results with active-GRASP supported the findings from GRASP. Stimulation with sucrose resulted in clear positive GRASP signal in the *Gr64f-lexA, Lk-Gal4 > active-GRASP* flies, whereas stimulation with water did not produce a positive result (**Figure 5B**). Similarly, caffeine stimulation produced a strong positive GRASP signal in the *Gr66a-LexA, Lk-Gal4 > active-GRASP* flies, that was absent in the control group (water) (**Figure 5D**) (see Materials and Methods for a full description of the stimulation procedure). Our GRASP and active-GRASP results indicate that SELK neurons receive active input from sweet $Gr64f^{GRNs}$ and bitter $Gr66a^{GRNs}$. Finally, we used BacTrace[50] to confirm that the connectivity between $Gr64f^{GRNs}$ and $Gr66a^{GRNs}$ neurons with SELK neurons is real. This technique works similarly to *trans*-Tango, but while *trans*-Tango labels postsynaptic neurons, BacTrace labels presynaptic partners. For our experiments, we used *Gr66a-LexA* and *Gr64f-LexA* as candidate presynaptic partners. Consistent with the GRASP and active-GRASP results, our BacTrace experiment indicated that sweet and bitter GRNs are presynaptic to SELK neurons (**Figure 5E**) further supporting a model in which Lk neurons are G2Ns receiving input from $Gr64f^{GRNs}$ and $Gr66a^{GRNs}$. To our best knowledge, this is the first time a G2N has been identified as collecting information from two populations of GRNs that transduce sensory information of different valence, sweet-attractive and bitter-repulsive.

Connectivity of SELK neurons within the Drosophila brain

Using molecular techniques, we have demonstrated that SELK neurons are G2Ns for both bitter $Gr66a^{GRNs}$ and sweet $Gr64f^{GRNs}$. We used the recently published Full Adult Fly Brain (FAFB) *Drosophila* connectome[51] to identify the SELK neurons and further analyze their connectivity. As SELK neurons receive simultaneous input from sweet and bitter GRNs, we took advantage of recent research that identified groups of bitter and sweet-sensing GRNs and their projections to the SEZ in the *Drosophila* brain connectome (**Sup. Figure 6A**)[24]. Using this dataset, we identify all postsynaptic partners to the $Gr64f^{GRNs}$ and $Gr66a^{GRNs}$ characterized, without limiting the number of synaptic contacts among neurons. We noted

12594 postsynaptic hits for Gr66a^{GRNs} and 36790 hits for Gr64f^{GRNs}. By intersecting both datasets, we obtained 333 downstream segment IDs as possible G2Ns receiving inputs from both GRNs. We refined our list to 17 candidates through visual inspection, focusing on neurons with projections within the SEZ (**Sup. Figure 6B**). To identify the SELK neuron among our candidates, we used the CMTK plugin in imageJ to register the immunohistochemistry images of the *Lk-Gal4* > *UAS-CD8::GFP* brains (**Figure 3A**) to a *Drosophila* reference brain (JRC2018U). Further, we skeletonized the images with ImageJ and uploaded them to the Flywire Gateway platform to compare the structure of the aligned SELK neurons with our candidates (**Sup. Figure 6C**). Via comparison with our candidates, we identified one candidate ID 720575940630808827 (GNG.685) (**Sup. Figure 6D**), which shared similar morphologies and projections to the right SELK neuron. The GNG.685 has a mirror twin, GNG.595, in the SEZ, and both are annotated as DNg68 in the Flywire database (**Figure 6A**). These candidates are classified as descending neurons, characteristic of known SELK neurons[38] and possibly also expressing the neurotransmitter acetylcholine. We consider the neurons DNg68 are the strongest candidates for representing SELK neurons (see Materials and Methods for a more detailed description).

To further analyze the connectivity of these neurons, we looked for the pre- and postsynaptic organization of SELK neurons. We only considered those synaptic partners with ≥10 synaptic connections to limit possible false positive synaptic connections. Most of the postsynaptic partners of SELK neurons (57) localized in the SEZ, as revealed by the BrainCircuits analysis[52] (**Figure 6B**), with significant projections to the pars intercerebralis. This region contains Insulin Producing Cells (IPCs) that project to the tritocerebrum in the SEZ, where a significant concentration of fibers can be appreciated in the *trans*-Tango immunohistochemistry (**Figure 6C**). This data supports previous results showing that IPCs express the *Lk receptor* (*Lkr*) and that they may be modulated by Lk-expressing neurons[40,44]. We found five bitter (GRN R1#4, GRN R1#5, GRN R1#12, GRN R2#1 and GRN R2#2) and three sweet (GRN R4#17, GRN R5#12 and GRN R5#14) GRN as presynaptic candidates to GNG.685 (right SELK neuron), and only one bitter (GRN R1#1) and one sweet (GRN R4#11) GRN as presynaptic candidates to GNG.595 (left SELK neuron) (IDs correspond to GRNs described in Engert et al., 2022[24]; Virtual Fly Brain) .That so few presynaptic GRNs were found indicates that SELK proofreading is still required for a much more precise assembly and annotation of the FAFB dataset. We identified a total of 101 presynaptic partners using BrainCircuits with a complex distribution over the brain (**Figure 6D**), though most of the connectivity was found within the SEZ. Additionally, we used *retro*-Tango[53], a retrograde trans-synaptic technique that employs similar trans-synaptic mechanisms as *trans*-Tango but in the retrograde direction. This experiment showed that SELK neurons receive most of the presynaptic input from neurons located in the SEZ (**Figure 6E**), consistent with the data

derived from the FAFB analysis. Encouragingly, we observed a significant concentration of synapsis at the tritocerebrum, similar to the *trans*-Tango signal.

Leucokinin modulates feeding behavior

We have shown that Lk neurons receive direct input from gustatory receptor neurons (GRNs) for bitter ($Gr66a^{GRNs}$) and sweet ($Gr64f^{GRNs}$), with Lk neuropeptide expression influenced by the animal's starvation level. Given that $Gr64f^{GRNs}$ facilitate feeding while $Gr66a^{GRNs}$ inhibit it, we sought to understand how Lk neurons integrate gustatory and metabolic signals to modulate feeding behavior. Previous studies indicated that silencing Lk neurons impaired flies' responses to sucrose in a Proboscis Extension Response (PER) experiment[40]. We silenced all Lk neurons in *Drosophila* using the *Lk-Gal4* driver to express the tetanus toxin (TNT) using the *UAS-TNT* driver alongside *UAS-TNT*^{imp} controls[54], then assessed their response in a PER assay (**Figure 7A**). The light chain of the tetanus toxin expressed with the *UAS-TNT* transgene, blocks all chemical transmission by cleaving the presynaptic protein nSyb. Unexpectedly, silencing Lk neurons did not change the gustatory response to varying sucrose concentrations in 24-hour starved flies (**Figure 7B**). Discrepancies with previous findings may stem from differences in handling and stimuli methodologies[40].

We hypothesized that Lk neurons might be important for processing sweet and bitter information. To test their role in the PER response to sweet food laced with bitter compounds, we combined 50 mM sucrose with increasing caffeine levels. It is known that *Drosophila* PER to a certain sucrose concentration decreases proportionally to the amount of a bitter compound (i.e. caffeine) it contains[2] (**Figure 7A**, Experiment 2). The PER experiments included fed, 12-hour, and 24-hour starved flies (**Figure 7C**). Fed flies showed a minimal response to 50 mM sucrose, with caffeine reducing this response consistently across both control and experimental groups. Twelve-hour starved flies exhibited stronger reactions to sucrose than fed flies, with caffeine diminishing PER in a concentration-dependent manner. Twenty four-hour starved flies showed larger PER values that decreased proportionally to the concentration of caffeine. However, this decrease was significantly larger when Lk neurons were silenced using TNT, indicating that Lk neurons are needed to tolerate and feed on food containing bitter, and potentially toxic, compounds. To restrict *Lk-Gal4* transgene expression, we employed the *tsh-Gal80*[55] construct, which is expressed in the Ventral Nerve Cord (VNC) to restrict Gal4 expression in this region. Restricting TNT expression to SELK and LHLK neurons, did not alter the previously observed PER responses to sweet and bitter compounds (**Sup**. **Figure 7A**). To investigate the role of Leucokinin further, we employed an RNAi line designed to knock-down Leucokinin production in Lk-expressing neurons. The results presented in **Sup. Figure 7B** demonstrate that knocking-down Leucokinin significantly

diminishes the flies' tolerance to caffeine in sweet food, indicating that this neuropeptide might be involved in the integration of sweet and bitter signals in Lk neurons.

Finally, we examined whether Lk neurons influence sustained feeding using the flyPAD[56] to monitor feeding behavior over one hour. We designed two feeding assays (**Figure 7D**). In Experiment 1, flies chose between 20 mM and 100 mM sucrose food. Typically, flies prefer higher sucrose concentrations, but if the higher concentration is mixed with a bitter compound (e.g., caffeine), acceptance of the lower concentration correlates with caffeine levels. Flies with silenced Lk neurons slightly preferred the higher sucrose concentration to controls (**Figure 7E**), yet caffeine addition did not affect their choices. The ingestion amounts for each fly remained comparable in both scenarios. Our findings indicate that Lk neurons are needed to tolerate and initiate feeding of food laced with bitter compounds; however, their role in sustained feeding remains unclear.

Discussion

We have demonstrated that Gustatory Second-Order Neurons (G2Ns), which transduce opposing behaviors such as sweet attraction and bitter repulsion, exhibit molecular differences and undergo transcriptomic changes upon starvation. Molecular, connectomic, and behavioral experiments have identified SELK neurons as particularly dynamic G2Ns when under starved conditions. Surprisingly, we discovered that these neurons simultaneously collect information from sweet-sensing Gr64f^{GRNs} and bitter-sensing Gr66a^{GRNs}. Additionally, SELK neurons respond to starvation by increasing the neuropeptide Leucokinin (Lk) expression. These findings reveal that Leucokinin neurons play a novel role in modulating feeding initiation during starvation when flies are presented with sweet food laced with bitter compounds.

Our RNAseq data analysis revealed that SELK neurons only received input from Gr66a^{GRNs}. However, further analysis using immunohistochemistry (*GRN-Gal4 > trans-Tango* + Lk immunohistochemistry) combined with GRASP, active-GRASP and BacTrace, demonstrated that SELK neurons are G2Ns to Gr64f^{GRNs} and Gr66a^{GRNs}. To our knowledge, this is the first demonstration that a pair of G2Ns are broadly tuned to both bitter and sweet gustatory inputs while also integrating metabolic information (**Figure 8A**). *trans*-Tango and its variants have been successfully used to study connectivity and functionality in various neuronal circuits, including gustatory, olfactory, visual systems, mushroom body output neurons or clock neurons[25,57–60]. Recent analysis of the *retro*-Tango tool, showed that a minimum number of synaptic connections between neurons is needed to label the postsynaptic neurons properly. It is possible that Gr64f^{GRNs} make fewer synaptic contacts with SELK neurons than Gr66a^{GRNs}, decreasing the probability of being labeled by *trans*-Tango.

Combined with our stringent FACS protocol, could explain why we were unable to capture SELK neurons as Gr64f^{G2Ns} with FACS.

Current understanding suggests that tastant quality is mediated by labeled lines, where gustatory receptor neurons are segregated to respond to specific taste qualities[61]. This segregation is thought to persist further upstream in the circuit, as observed in mice, where taste cells respond to specific tastants, and this information remains segregated at the geniculate ganglion[62], gustatory cortex[63], and the amygdala[64]. Similarly, in *Drosophila* GRNs that detect bitter and sweet compounds project their axons to the SEZ in a non-overlapping fashion[10]. Whole-brain *in vivo* calcium imaging revealed that most SEZ interneurons respond to single tastants[65]. However, the same study identified neurons that may respond to multiple tastants, like bitter and sweet, though specific neurons and their circuit positions were not detailed. Other SEZ neurons have been shown to integrate sweet and bitter inputs, such as the E49 motor neuron, which is stimulated by sweet input (Gr5a) and inhibited by bitter input (Gr66a)[66], but these are not G2Ns. We attempted *in vivo* calcium imaging to further study the gustatory integration in those neurons, but we were unsuccessful due to the challenging location of SELK somas in the medio-ventral region of the SEZ, which is obscured by the proboscis even when fully extended. Additionally, variability in labeling using *UAS-GCaMP7s*, *UAS-GCaMP7m* and *UAS-GCaMP6f* lines hampered the proper imaging of these neurons. Our behavior experiments show that Leucokinin neurons (most likely SELK neurons) are early integrators of gustatory and metabolic information.

In summary, our study highlights the complex integration of gustatory and metabolic information by Leucokinin neurons, providing new insights into the neural mechanisms underlying feeding behavior in *Drosophila*. This work advances our understanding of how sensory and metabolic cues are integrated into the brain to regulate vital behaviors such as feeding.

Acknowledgments

We thank Prof. Richard Benton, Prof. Roman Arguello, and members of the JSA laboratory for their comments on the manuscript. We also thank our colleagues from the Institute of Neuroscience (IN) for their insightful inputs while developing the present research. This work was funded by the Spanish State Research Agency (AEI/10.13039/501100011033), operating grants PID2019-105839GA-I00, CNS2022-135109, “Ramón y Cajal” Fellowship RyC2019-026747-I and “Severo Ochoa” Centre of Excellence grant to the IN (grant CEX2021-001165-S).

Author contribution

JSA conceived the project and wrote the manuscript with RMA. JSA and RMA performed the brain dissections for the RNAseq analysis. RMA did the FACS sorting, RNA extraction, and sample preparation for sequencing. JSA performed the RNAseq analysis. RMA did the immunohistochemistry, connectomic analysis and PER behavior. MJC performed the flyPAD experiments.

Declaration of interests

The authors declare no competing interests.

Main figures and figure legends

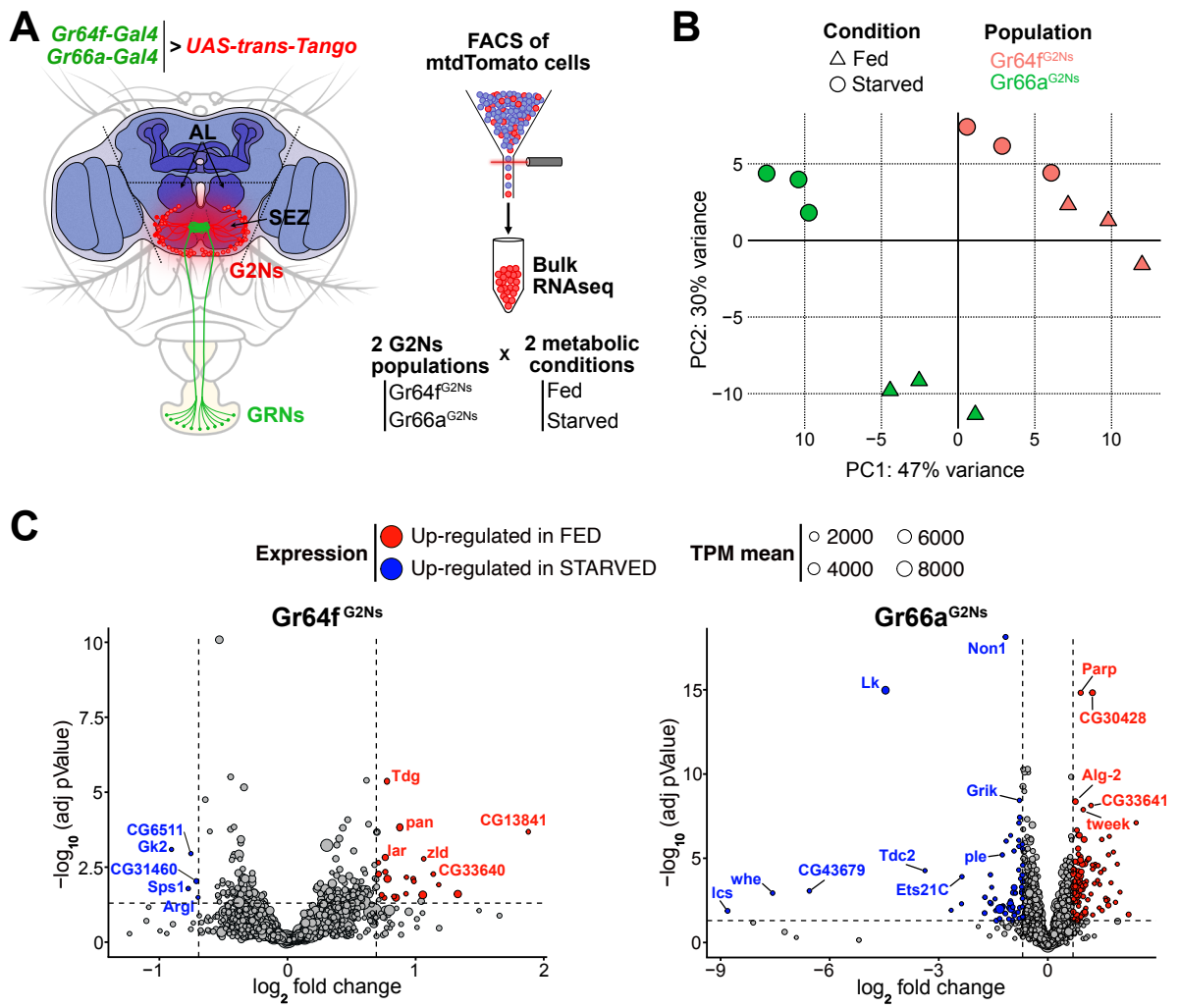

Figure 1. **The metabolic state affects the gene profiles of the Gustatory Second-Order Neurons (G2Ns) populations analyzed**. (**A**) The scheme depicts the region of the brain dissected and the sorting of the G2Ns according to the input. Two populations of *trans*-Tango neurons were labeled using *Gr64f-Gal4* and *Gr66a-Gal4* transgenic lines. Flies were either fed or food-starved for 24 hours. (**B**) Principal Component Analysis (PCA) of the genes. (**C**) Volcano plots show the genes up- and down-regulated in fed and starved conditions in the two populations of G2Ns.

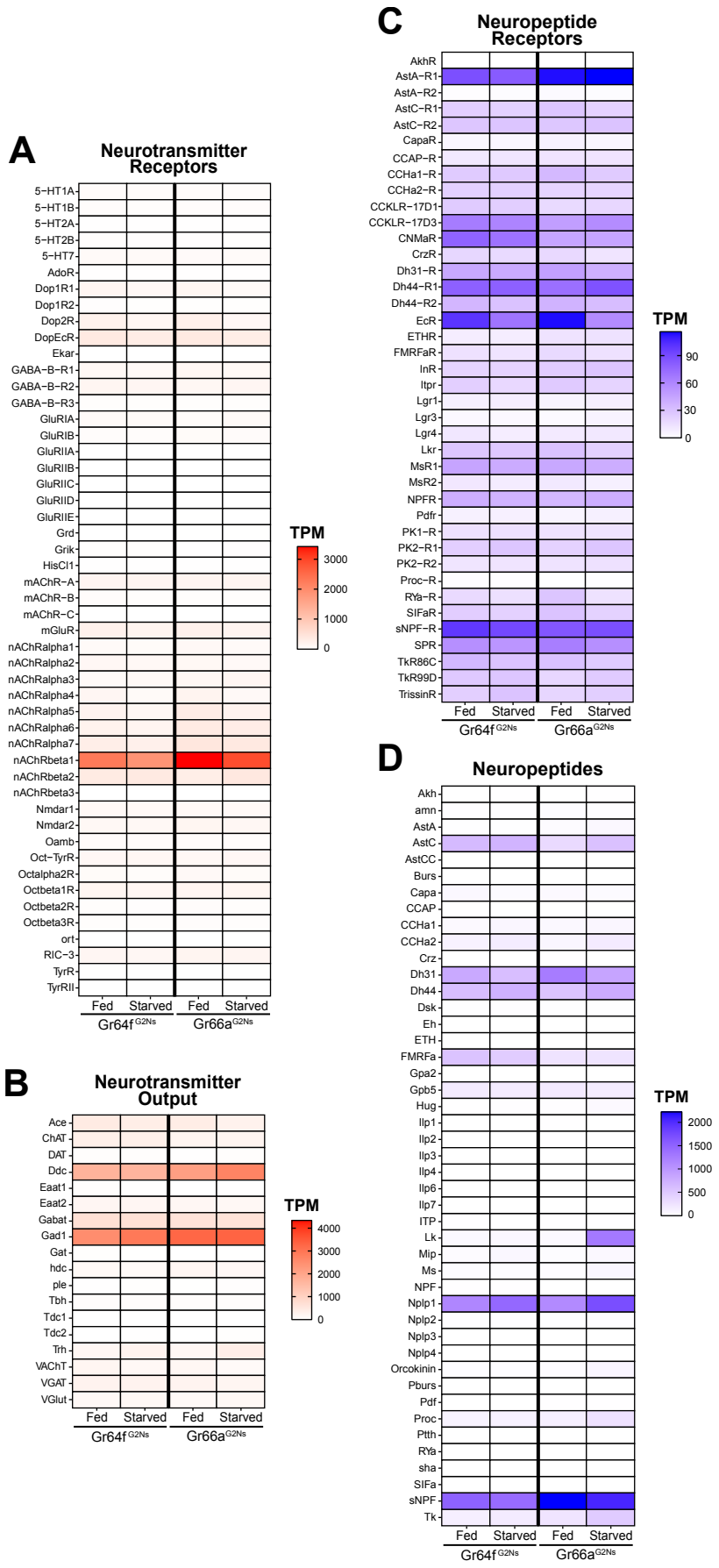
A
Neurotransmitter Receptors
5-HT1A
5-HT1B
5-HT2A
5-HT2B
5-HT7
AdoR
Dop1R1
Dop1R2
Dop2R
DopEcR
Ekar
GABA-B-R1
GABA-B-R2
GABA-B-R3
GluRIA
GluRIB
GluRIIA
GluRIIB
GluRIIC
GluRIID
GluRIIE
Grd
Grik
HisCl1
mAChR-A
mAChR-B
mAChR-C
mGluR
nAChRalpha1
nAChRalpha2
nAChRalpha3
nAChRalpha4
nAChRalpha5
nAChRalpha6
nAChRalpha7
nAChRbeta1
nAChRbeta2
nAChRbeta3
Nmdar1
Nmdar2
Oamb
Oct-TyrR
Octalpha2R
Octbeta1R
Octbeta2R
Octbeta3R
ort
RIC-3
TyrR
TyrRII
Fed
Starved
Fed
Starved
Gr64f G2Ns
Gr66a G2Ns
TPM
3000
2000
1000
0
B
Neurotransmitter Output
Ace
ChAT
DAT
Ddc
Eaat1
Eaat2
Gabat
Gad1
Gat
hdc
ple
Tbh
Tdc1
Tdc2
Trh
VAChT
VGAT
VGlut
Fed
Starved
Fed
Starved
Gr64f G2Ns
Gr66a G2Ns
TPM
4000
3000
2000
1000
0
C
Neuropeptide Receptors
AkhR
AstA-R1
AstA-R2
AstC-R1
AstC-R2
CapaR
CCAP-R
CCHa1-R
CCHa2-R
CCKLR-17D1
CCKLR-17D3
CNMaR
CrzR
Dh31-R
Dh44-R1
Dh44-R2
EcR
ETHR
FMRFaR
InR
Itpr
Lgr1
Lgr3
Lgr4
Lkr
MsR1
MsR2
NPFR
Pdfr
PK1-R
PK2-R1
PK2-R2
Proc-R
RYa-R
SIFaR
sNPF-R
SPR
TkR86C
TkR99D
TrissinR
Fed
Starved
Fed
Starved
Gr64f G2Ns
Gr66a G2Ns
TPM
90
60
30
0
D
Neuropeptides
Akh
amn
AstA
AstC
AstCC
Burs
Capa
CCAP
CCHa1
CCHa2
Crz
Dh31
Dh44
Dsk
Eh
ETH
FMRFa
Gpa2
Gpb5
Hug
Ilp1
Ilp2
Ilp3
Ilp4
Ilp6
Ilp7
ITP
Lk
Mip
Ms
NPF
Nplp1
Nplp2
Nplp3
Nplp4
Orcokinin
Pburs
Pdf
Proc
Ptth
RYa
sha
SIFa
sNPF
Tk
Fed
Starved
Fed
Starved
Gr64f G2Ns
Gr66a G2Ns
TPM
2000
1500
1000
500
0

Figure 2. **Transcripts per Million (TPM) for Neuropeptides and Neurotransmitters**. TPMs for Neurotransmitters (**A**), Neurotransmitter Receptors (**B**), Neuropeptides (**C**) and Neuropeptide Receptors (**D**) for the two G2N populations in the two metabolic conditions studied (fed and 24h starved).

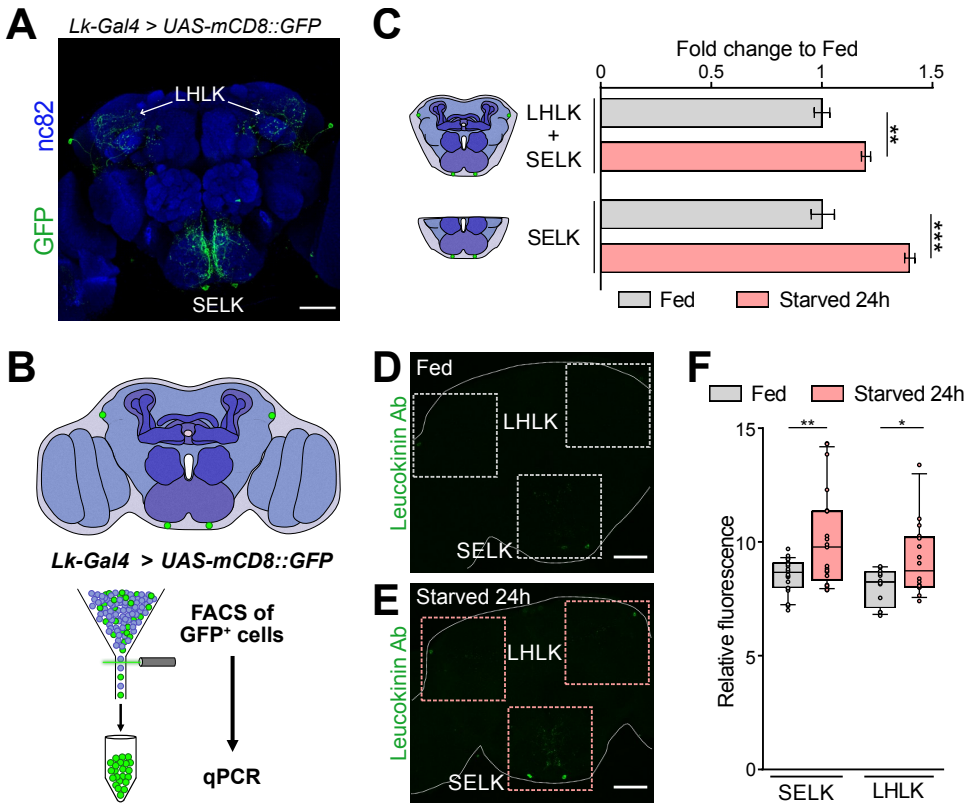

Figure 3. ***Leucokinin* expression is increased in starvation**. (**A**) Immunofluorescence with anti-GFP (green) and anti-nc82 (blue) on a whole-mount brain of a *Lk-Gal4 > UAS-mCD8::GFP*. (**B**) Scheme showing the approach used to select the Lk GFP$^+$ neurons by FACS. (**C**) qPCR results for Lk neurons labeled with GFP and sorted by FACS. The central brain includes four Lk neurons, while the SEZ region includes only the two neurons located in this region. (**D**) Intensity fluorescence quantification in whole *Oregon-R* brains stained with anti-Lk antibody in fed and 24-hour starved flies. SELK Fed = 20 brains; SELK Starved = 21 brains; LHLK Fed = 12 brains; LHLK Starved = 16 brains. Statistical test: Wilcoxon rank sum test. *$p<0.05$, **$p<0.01$, ****$p<0.0001$. Scale bar = 50 μm.

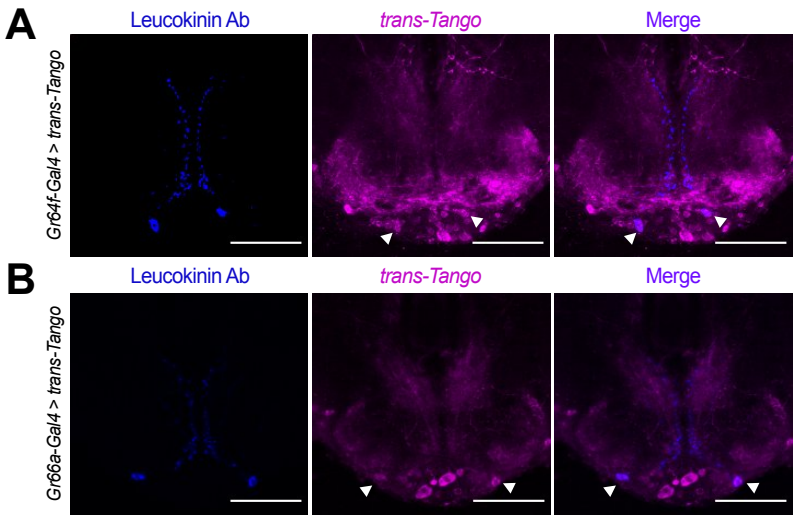

Figure 4. Lk neurons co-localize with the *trans*-Tango signal. Immunofluorescence with anti-Leucokinin (blue) and anti-RFP (magenta) on whole-mount brains of (**A**) *Gr64f-Gal4* > *trans-Tango*, and (**B**) *Gr66a-Gal4* > *trans-Tango*. Images correspond to the adult SEZ. Arrowheads point to SELK neurons. Scale bar = 50 μm.

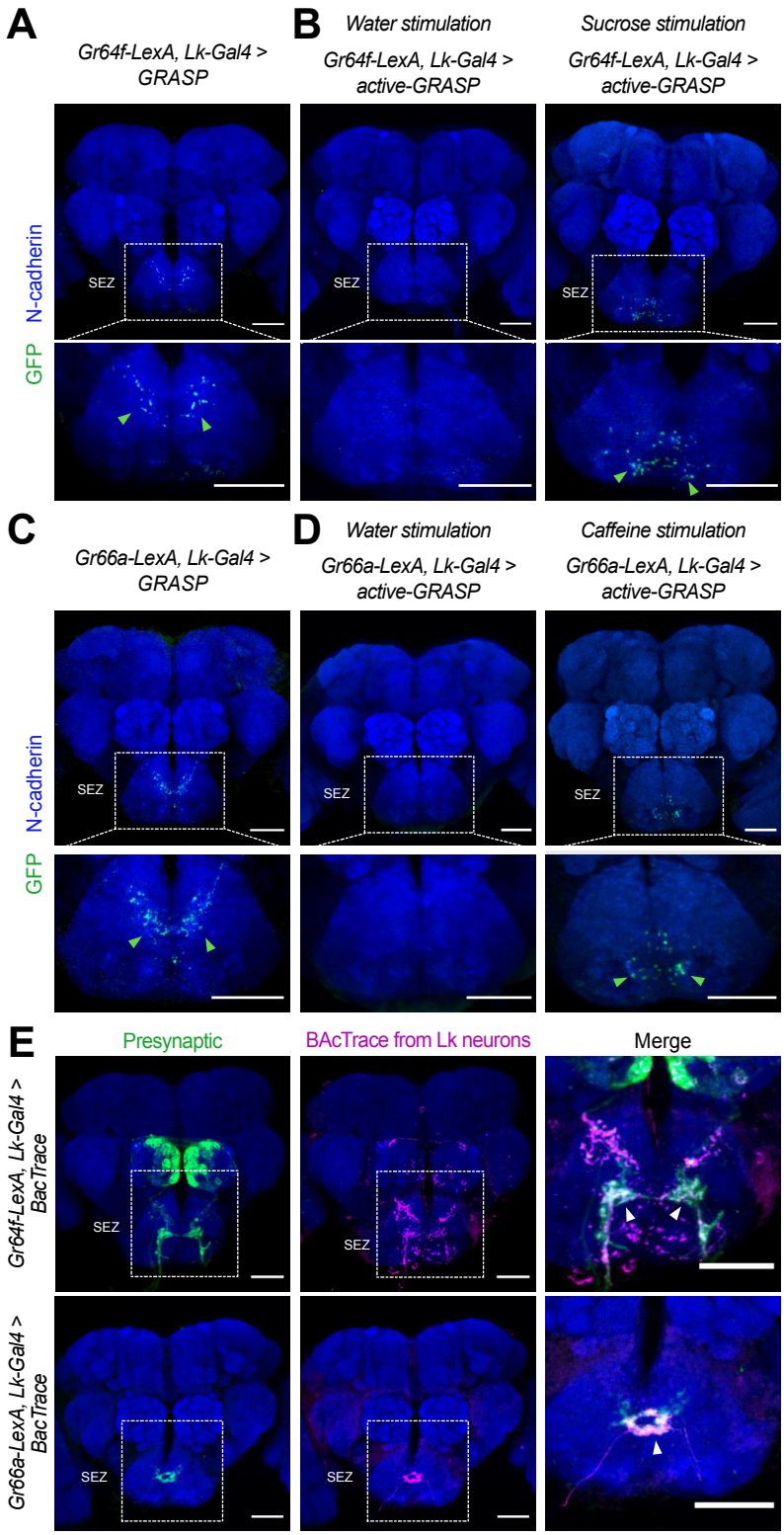

Figure 5. Lk neurons are synaptically connected to Gr64f^{GRNs} and Gr66a^{GRNs}. (**A**) **GRASP:** Immunofluorescence with anti-GFP (green) and anti-N-cadherin (blue) on whole-mount brains of *Gr64f-LexA > LexAop-CD4spGFP^{11}* and *Lk-Gal4 > UAS-CD4spGFP$^{1-10}$* flies. (**B**) **Active-GRASP**: Immunofluorescence with anti-GFP (green) and anti-N-cadherin (blue) on whole-mount brains of *Gr64f-LexA > LexAop-nSybspGFP$^{1-10}$* and *Lk-Gal4 > UAS-CD4spGFP^{11}*

stimulated with water (left column) and sucrose (right column). (**C**) **GRASP:** Immunofluorescence with anti-GFP (green) and anti-N-cadherin (blue) on whole-mount brains of *Gr66a-LexA* > *LexAop-CD4spGFP*^{11} and *Lk-Gal4* > *UAS-CD4spGFP*$^{1-10}$. (**D**) **Active-GRASP**: Immunofluorescence with anti-GFP (green) and anti-N-cadherin (blue) on whole-mount brains of *Gr66a-LexA* > *LexAop-nSybspGFP*$^{1-10}$ and *Lk-Gal4* > *UAS-CD4spGFP*^{11} stimulated with water (left column) and caffeine (right column). (**E**) Immunofluorescence with anti-GFP (green), anti-RFP (magenta), and anti-nc82 (blue) on whole-mount brains of *Gr64f-LexA, Lk-Gal4* > *BacTrace* (top row) and *Gr66a-LexA, Lk-Gal4* > *BacTrace* (bottom row). Arrowheads point to the BacTrace positive signal. Scale bar = 50 μm.

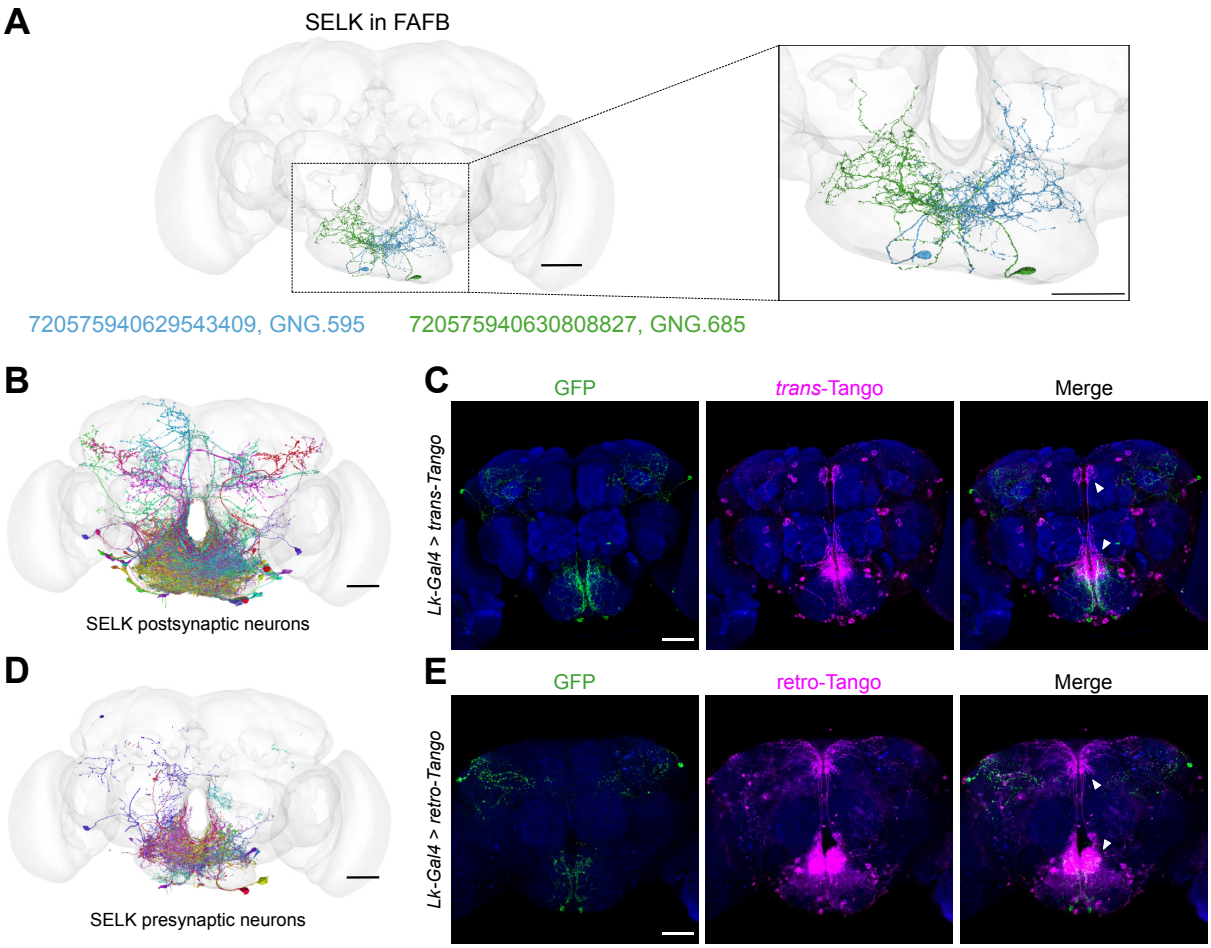

Figure 6. Lk neurons are pre- and postsynaptic to a significant number of neurons. (**A**) The anatomy of the SELK neurons (Right in green and Left in blue) was reconstructed using the FAFB brainmesh template in Flywire. IDs from Flywire are indicated: 720575940629543409 ID for the Left SELK in blue (GNG.595/DNg68(L)) and 720575940630808827 for the Right SELK in green (GNG.685/DNg68(R)). Zoom in to the SEZ from (**A**), showing the details of the neuronal arborizations. (**B**) SELK postsynaptic candidate neurons reconstructed in the FAFB (Full Adult Fly Brain) brainmesh template in Flywire. Only postsynaptic candidate neurons with ≥10 synaptic points with SELK neurons are shown (57 postsynaptic candidate neurons). (**C**) Immunofluorescence with anti-GFP (green), anti-RFP (magenta), and anti-nc82 (blue) on a whole-mount brain on a *Lk-Gal4 > trans-Tango* flies. (**D**) SELK presynaptic candidate neurons reconstructed in the FAFB brainmesh template in Flywire. Only presynaptic candidate neurons with ≥10 synaptic points with SELK neurons are shown (101 presynaptic candidate neurons). (**E**) Immunofluorescence with anti-GFP (green), anti-RFP (magenta), and anti-nc82 (blue) on a whole-mount brain on a *Lk-Gal4 > retro-Tango* flies. Scale bar: 50 µm.

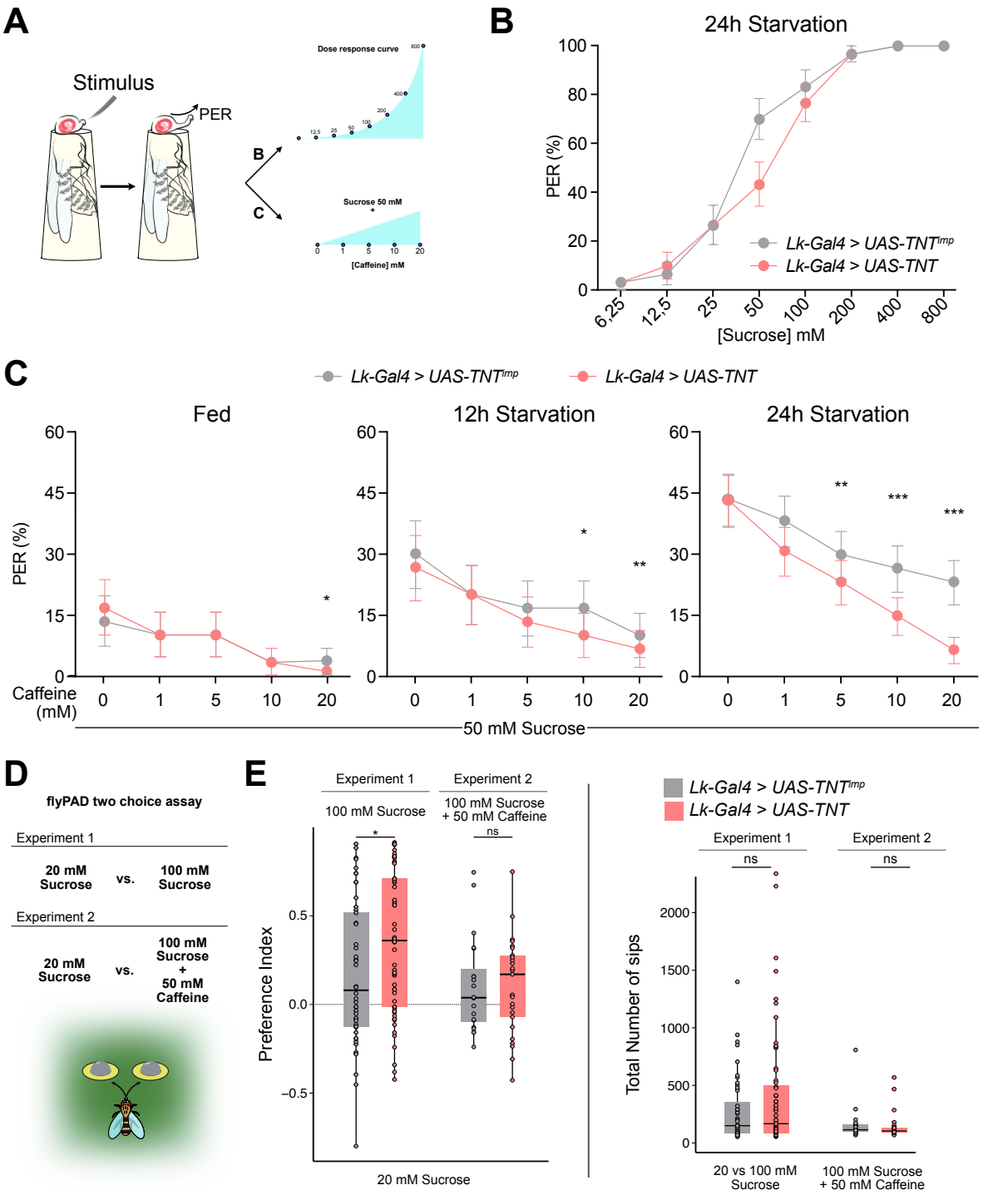

Figure 7. Leucokinin neurons integrate sweet and bitter gustatory information. (**A**) Scheme depicting the experimental procedure for Proboscis Extension Reflex (PER). Flies are given a series of increasing concentrations of sucrose (6.25, 12.5, 25, 50, 100, 200, 400 and 800 mM) for Experiment 1; and a fixed concentration of sucrose (50 mM) mixed with increasing concentrations of caffeine (1, 5, 10 and 20 mM) for Experiment 2. All flies starved 24 hours. (**B**) PER dose response curve of *Lk-Gal4 > UAS-TNT*^{imp} (n=30) and *Lk-Gal4 > UAS-*

TNT (n=30) flies for Experiment 1. (**C**) PER of *Lk-Gal4* > *UAS-TNT*^{imp} (n=30) and *Lk-Gal4* > *UAS-TNT* (n=30) flies for Experiment 2. (**D**) Scheme depicting the experimental procedure for flyPAD (Adapted from Itskov et al., 2014[56]). Experiment 3: 20 mM Sucrose vs. 100 mM Sucrose and Experiment 4: 20 mM Sucrose vs. 100 mM Sucrose + 50 mM Caffeine. All flies starved 24 hours. (**E**) Preference Index (Left) for the highest concentration of sucrose (100 mM) with or without 50 mM caffeine and total number of sips (Right) for Experiment 3 and 4. Experiment 3: *Lk-Gal4* > *UAS-TNT*^{imp} (n=48); *Lk-Gal4* > *UAS-TNT* (n=59); Experiment 4: *Lk-Gal4* > *UAS-TNT*^{imp} (n=20); *Lk-Gal4* > *UAS-TNT* (n=25). Only flies that performed a minimum of 25 sips per fly and 2 bouts were considered for the analysis. ns: non-significant, *$p<0.05$. PER analysis: Logistic regression model with binomial distribution; Error bars represent the standard error of the proportion. flyPAD statistics Wilcoxon Rank Sum Test.

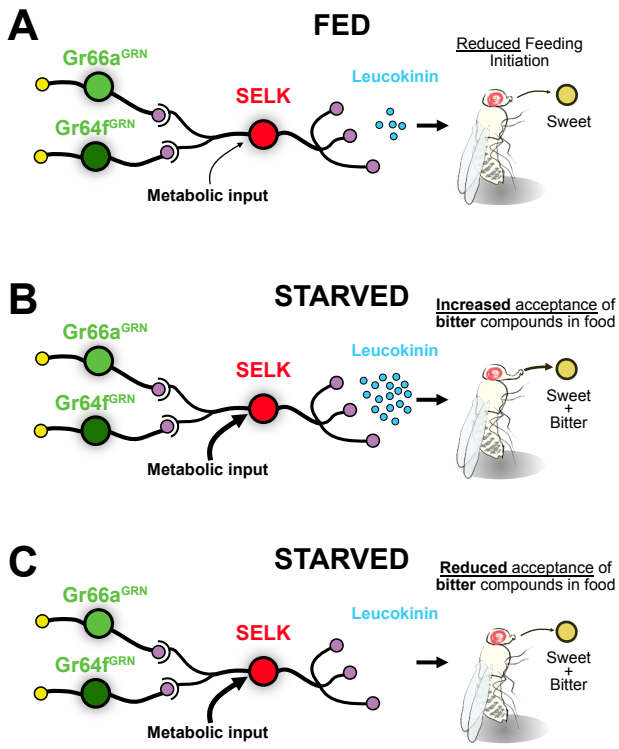

Figure 8. Model for the integration of gustatory information by SELK neurons. (**A**) SELK neurons receive direct input from Gr64f^{GRNs} (sweet), Gr66a^{GRNs} (bitter), and metabolic information. When flies are fed, the expression of the neuropeptide Leucokinin is reduced. The probability of a fed fly initiating feeding is reduced when facing any food. (**B**) SELK neurons in starved flies express large amounts of Leucokinin. In this situation, flies are more prone to accept food containing bitter compounds. (**C**) Starved flies with silenced SELK neurons are less prone to accept sweet foods laced with bitter compounds.

Materials and Methods

Key Resource Table

***Drosophila* strains**	**Source**		**Identifier**
Oregon-R	Kindly donated by Prof. Richard Benton		NA
w^{1118}	Kindly donated by Prof. Francisco Tejedor		NA
Gr64f-Gal4	Kindly donated by Prof. Richard Benton		NA
Gr64f-LexA	Kindly donated by Prof. Richard Benton		NA
Gr66a-Gal4	Bloomington *Drosophila* Stock Center		BDSC 57670
Gr66a-LexA; LexAop-rCD2::GFP	Kindly donated by Prof. Richard Benton		NA
Lk-Gal4 (2nd Chr)	Bloomington *Drosophila* Stock Center		BDSC 51993
Lk-Gal4 (X Chr) used only in tsh-Gal80 experiment	Bloomington *Drosophila* Stock Center		BDSC 51992
QUAS-mtdTomato; retro-Tango; UAS-retro-Tango-GFP (*retro-*Tango)	Bloomington *Drosophila* Stock Center		BDSC 99661
UAS-mCD8::GFP	Bloomington *Drosophila* Stock Center		BDSC 32186
UAS-myrGFP, QUAS-mtdTomato; trans-Tango (*trans-*Tango)	Bloomington *Drosophila* Stock Center		BDSC 77124
UAS-TNT	Bloomington *Drosophila* Stock Center		BDSC 28837
UAS-TNT^{imp}	Bloomington *Drosophila* Stock Center		BDSC 28839
UAS-RNAi^{Lk}	Bloomington *Drosophila* Stock Center		BDSC 25798
UAS-CD4-spGFP1-10, lexAop-CD4-spGFP11 (GRASP)	Bloomington *Drosophila* Stock Center		BDSC 58755
lexAop-nSyb-spGFP1-10, UAS-CD4-spGFP11; MKRS/TM6B (Active GRASP)	Bloomington *Drosophila* Stock Center		BDSC 64315
LexAop-GFP, LexAop-QF; UAS-B3RT, QUAS-mtdTomato (BAcTrace)	Bloomington *Drosophila* Stock Center		BDSC 90826
tsh-Gal80	Kindly donated by Prof. María Domínguez		
Primary antibodies	**Host species**	**Source**	**Working dilution**
Green Fluorescent Protein (GFP)	Chicken	Abcam (ab13970)	1:500
Red Fluorescent Protein (RFP)	Rabbit	Abcam (ab62341)	1:500
nc82 Bruchpilot	Mouse	DSHB	1:50
GFP reconstructed in GRASP	Mouse	Sigma-Aldrich (G6539)	1:500
Leucokinin	Rat	Kindly donated by Prof. Pilar Herrero	1:100

Cadherin DN-Extracellular Domain	*Rat*	Jackson Inmunoresearch 112-165-003	1:500
Secondary Antibodies	**Host species**	**Source**	**Working dilution**
Anti-Chicken Alexa 488	Goat	Abcam (ab150169)	1:250
Anti-Rabbit Cy3	Goat	Jackson Inmunoresearch 111-165-144	1:250
Anti-Mouse Cy5	Goat	Jackson Inmunoresearch 115-175-146	1:250
Anti-Mouse Cy3	Goat	Jackson Inmunoresearch 115-165-166	1:250
Anti-Mouse Alexa 488	Goat	Jackson Inmunoresearch 115-545-003	1:250
Anti-Rat Cy3	Goat	Jackson Inmunoresearch 112-165-167	1:250
Anti-Rat Alexa 697	Goat	Jackson Inmunoresearch 112-605-167	1:250
Chemicals	**Source**		**Reference**
Sucrose	Sigma Aldrich		102174662
Caffeine	Sigma Aldrich		102143502
Agarose	Condalab		8100.00
Agarose (low melting)	Lonza		50100

Drosophila **husbandry**

Drosophila melanogaster stocks were reared and maintained on standard “Iberian” fly food under a 12 h light:12 h dark cycle at 25 ºC. w^{1118} and *Oregon-R* fly lines were used as mutant and wild-type strain controls unless otherwise indicated. Starvation was induced by transferring flies into vials containing a solid medium formed with a piece of paper (Kimberly-Clark Kimtech, ref. 7552) soaked with 2,5 ml tap water. All *Drosophila* strains used in this thesis are listed in the Key Resource Table.

Tissue dissection and Fluorescence Activated Cell Sorting (FACS)

Central Brains or SEZs were dissected in cold Calcium- and Magnesium-free 1X Dulbecco’s Phosphate Buffered Saline (DPBS) (ThermoFischer, ref. 14190094), transferred to a Protein LoBind (Eppendorf, ref. 0030108116) tube containing DPBS 0.01% BSA (Bovine Serum Albumin) (Invitrogen, ref. AM2616) and digested with 1 mg/ml of papain and collagenase (Sigma-Aldrich, ref. P4762 and C2674, respectively). After enzymatic digestion, dissociated tissue solution was filtered through a 20 µm filter (pluriSelect, ref. SKU 43-10020-40) into 300

µl DPBS BSA 0.01% in a Protein LoBind tube. Samples were kept at -80ºC or directly sorted by FACS.

Cells were sorted using a FACS AriaTM III. Several steps were followed to discard debris, clustered cells and dead cells using a DAPI fluorescent filter. Gustatory Second Order Neurons labeled with mtdTomato were selected using a 555 nm laser (RFP PE-Texas Red A) to discard non-fluorescent cells from the red fluorescent population. In addition to the 555 nm laser, to differentiate those autofluorescence (far red, λ > 670 nm) from actual mtdTomato *trans*-Tango signal from gustatory second-order neurons (λ = 615 nm), a far red 566 nm laser (PE-Cy7-A) was applied consecutively to only conserve those mtdTomato fluorescent single cells for PE-Texas Red-A laser and not for PE-Cy7-A laser. All fluorescent gustatory second order neurons were sorted into Protein LowBind RNase-free tubes containing 15 µl of lysis buffer for RNA extraction and finally stored at -80ºC. To sort the Lk GFP^+ neurons the 488 nm laser was used to sort only GFP^+ fluorescent cells by applying the FITC-A filter.

Table 1. Number of brains and cells dissected

Fed Flies			Starved Flies		
Replicate	**#Brains dissected**	**#Cells collected**	**Replicate**	**#Brains dissected**	**#Cells collected**
Gr64f_1	406	21017	**Gr64f_1**	372	23126
Gr64f_2	512	23782	**Gr64f_2**	315	23387
Gr64f_3	191	21428	**Gr64f_3**	459	23267
Gr66a_1	519	21260	**Gr66a_1**	657	27555
Gr66a_2	531	21599	**Gr66a_2**	718	27090
Gr66a_3	594	21433	**Gr66a_3**	636	26991

RNAseq analysis

RNA extraction and sequencing

RNA was extracted using the PicoArcturus RNA isolation kit (ThermoFisher, ref. 12204-01). The spectrophotometer NanoDrop® ND-1000 was used for samples estimated to contain higher amounts of total mRNA extracted, in the range of 100-3.000 ng/µl. Additionally, to obtain the exact concentration and test the mRNA's quality, total mRNA was measured using the 2100 Bioanalyzer (Agilent Technologies). 50 to 5.000 pg/µl range was measured using chips from the RNA 6.000 Pico Kit (Agilent Technologies).

Samples were sequenced using 50 bp single reads on an *Illumina HiSeq2500* (for fed condition) and *Illumina NextSEq2000* (for starved condition) sequencers at the Genomics Unit of the Center for Genomic Regulation (Barcelona, Spain).

Reads were quality-checked with MultiQC v1.0 software using the tool FastQC v0.11.9. RNAseq output reads were aligned to the *D. melanogaster* reference genome from the

Ensemble Project database (EMBL-EBI, Cambridge, UK) using STAR v2.7.9a (Spliced Transcripts Alignment to a Reference)[67]. Differential gene expression analysis was performed using DESeq2 v1.28.1[68] with the free *R* programming language (GNU project) software *RStudio* v4.2. Also, the reads within the gene were transformed by this tool to a total of counts per gene. Transcripts per million (TPM) were calculated using Salmon 1.10.2[69]. A combination of packages (or libraries) from CRAN and Bioconductor v3.14[70,71] open-source projects were used for data processing and plotting.

Gene Ontology analysis

The Gene Ontology (GO) analysis was performed using the open source interface PANGEA (Pathway, Network and Gene-set Enrichment Analysis; https://www.flyrnai.org/tools/pangea/)[72] specifically the *Drosophila* GO subsets terms at the online platform. Only those genes significantly up-regulated or significantly down-regulated in the differential gene expression analysis were included in the GO analysis. Each of the G2N's differential expressed genes was analyzed separately, and then, only those GO terms of interest were plotted in one single graph.

Additionally, other GO analysis interfaces and tools as g::Profiler (https://biit.cs.ut.ee/gprofiler/gost), AmiGO2 (https://amigo.geneontology.org/amigo) undefined were used to validate the results of PANGEA. Finally, Gene set enrichment analysis (GSEA) was represented using RStudio v4.2 software (code available upon request).

qPCR

Standard real-time quantitative PCR (qPCR) was performed with 2 ng of template cDNA, PowerUp SYBR Green PCR Master Mix (Applied Biosystems, ref. A25742) and gene-specific primers read on QuantStudio 3 Real-Time PCR System (Applied Biosystems, ref. A28567) with a standard cycling mode: 2 minutes at 50ºC and another 2 minutes at 95ºC followed by 40x cycles of 15 seconds at 95ºC and 1 minutes at 60ºC. *Gapdh2* (Glyceraldehyde 3 phosphate dehydrogenase 2) of *D. melanogaster* protein expression levels was used as a housekeeping gene to normalize the results. Triplicate samples per each condition and technical triplicates were performed, and the relative gene expression was normalized by ΔCt analysis. Data is presented as mean ± SEM, and was statistically analyzed using two-tailed Student's *t*-test, considering $p<0.05$ to be statistically significant. Primers used:

Gene	Forward sequence (5' to 3')	Reverse sequence (5' to 3')
LK[40]	GCCTTTGGCCGTCAAGTCTA	TGAACCTGCGGTACTTGGAG
Gapdh2[74]	CTACCTGTTCAAGTTCGATTCGAC	AGTGGACTCCACGATGTATTC

Immunohistochemistry

Immunofluorescence on peripheral and central tissues of adult flies was performed following standard procedures [75,76]. In brief, brains and proboscis were dissected in cold Phosphate Buffer (PB) and fixed for 25 minutes in 4% Paraformaldehyde (PFA EMS15710) in PB at RT. After that, brains and proboscis were washed 5 times for 10 minutes with PB + 0.3% Triton X-100 (PBT) and blocked for 1 hour in PBT + 5% normal goad serum (NGS) (Abcam, ref. ab7481). Later, primary and secondary antibody (see Key Resource Table) incubations were for 48hours each in PBT + 5% NGS at 4ºC in constant agitation. Finally, after 5 washes of 10 minutes, brains and proboscis were equilibrated and mounted in Vectashield Antifade Mounting Medium with DAPI (Vector Laboratories, ref. H-1200-10), maintaining their three-dimensional structure.

Active-GRASP stimulation

Sweet GRN stimulation

Pupae were selected and placed in tubes containing the desired stimuli to prevent adult flies from accessing our standard "Iberian" food which includes yeast and sucrose. *Gr64f-LexA, Lk-Gal4 > active-GRASP* pupae were transferred to tubes with a piece of paper (Kimberly-Clark Kimtech, ref. 7552) soaked in tap water (control group, no activation of $Gr64f^{GRNs}$) or to a vial containing paper saturated with a 200 mM sucrose solution (sucrose stimulation group, activation of $Gr64f^{GRNs}$). Adults were maintained in each condition for 48 hours at 25ºC until dissection.

Bitter GRN stimulation

Gr66a-LexA; Lk-Gal4 > active-GRASP 1 to 2-day-old adults were transferred into two different conditions: food with sucrose (control condition, no activation of $Gr66a^{GRNs}$) and food with sucrose and caffeine (bitter stimulation group, activation of $Gr66a^{GRNs}$). Adding sucrose to the food is necessary to induce the feeding of caffeine-containing food, as the bitter taste itself induces repulsion[10]. Female flies were maintained for 3-4 days in each condition until dissection.

- Sucrose food: 200 mM sucrose (Sigma Aldrich, ref. 102174662), miliQ water, 0,9% NaCl, 2,7% yeast and 1% agarose.
- Sucrose + caffeine food: 200 mM sucrose, 75 mM caffeine, miliQ water, 0,9% NaCl, 2,7% yeast and 1% agarose.

To enhance the stimulation of sweet and bitter GRNs, prior to dissection, flies were immobilized on P200 tips and the proboscis was exposed to a piece of paper (Kimberly-Clark Kimtech, ref. 7552) containing 1 M Sucrose (for *Gr64f-LexA, Lk-Gal4 > active-GRASP* flies)

and 75 mM Caffeine (for *Gr66a-LexA, Lk-Gal4 > active-GRASP* flies) for 1 hour in a humidified chamber. Following this, the flies were dissected according to the immunohistochemistry protocol.

Microscopy image capture and processing

Images were acquired using a Leica SPEII laser scanning confocal microscope. Routinely, images of dimensions 512x512 pixels were acquired using an oil immersion 20x objective in stacks of 1-2 µm. Files were saved in *.tiff* format and processed with ImageJ (Fiji) open-source image-processing software[77]. For fluorescence quantification, the fluorescent intensity from the Region Of Interest (ROI) area was analyzed by using the ROI Manager from ImageJ, and data is presented as mean ± standard error of the mean (SEM) and was statistically analyzed using two-tailed Student's *t*-test, considering $p<0.05$ to be statistically significant.

Identification of the SELK neurons in the adult brain *Drosophila* connectome

Neurons were reconstructed in a serial section transmission electron volume [51] using FlyWire (https://flywire.ai/) [78–80]. To accomplish this, 52 sweet and bitter GRNs skeletons (*.swc* format), previously described [24], were downloaded from the open-source interface of Virtual Fly Brain (VFB)[81] and aligned to the Full Adult Fly Brain (FAFB) using the JRC2018U reference brain as a template [51,82,83]. Among these, 19 GRNs were bitter sensing (12 from group 1 (**Sup. Figure 6A**) and seven from group 2 (**Sup. Figure 6B**)), while 33 GRNs were sweet sensing (17 from group 4 (**Sup. Figure 6C**) and 16 from group 5 (**Sup. Figure 6D**)). Only $Gr64f^{GRNs}$ and $Gr66a^{GRNs}$ from the right hemisphere were used in this analysis due to the larger dataset. All these GRN skeletons were aligned to the recently released FlyWire dataset, which is a dense, machine learning-based reconstruction of over 80,000 FAFB neurons [79]. Using the Flywire Gateway tool, each of the sweet and bitter GRNs analyzed was aligned and reconstructed to the EM dataset in the FlyWire toolbox, with the IDs annotated[78].

We next used BrainCircuits[52] to identify all postsynaptic partners to sweet $Gr64f^{GRNs}$ and bitter $Gr66a^{GRNs}$. The postsynaptic candidates were downloaded without limiting the number of synaptic contacts among neurons. We noted 12594 postsynaptic hits for $Gr66a^{GRNs}$ and 36790 hits for $Gr64f^{GRNs}$. By intersecting both datasets, we obtained 333 downstream segment IDs as potential G2Ns receiving inputs from both GRNs. We refined our list to 17 candidates through visual inspection, focusing on neurons with projections within the SEZ (**Table 2**).

Table 2. List of candidate IDs

Flywire IDs	Name
720575940604891360	
720575940637742150	
720575940624273149	

720575940624253991	
720575940635642725	
720575940633198284	
720575940647033396	
720575940635179871	
720575940606866377	
720575940631349335	
720575940629913130	
720575940632524559	
720575940613670893	
720575940630808827	**GNG.685**
720575940616353675	
720575940623476407	
720575940630456028	

In order to identify which of the 17 candidates presented in Table 2 correspond to the SELK neurons, we proceeded to register the SELK neurons in a reference brain template. To achieve this, immunohistochemistry was performed on 7-day-old *Lk-Gal4* > *UAS-CD8::GFP* flies using nc82 (to label the brain structure) and GFP (to label the SELK neurons). Images were taken at a resolution of 1024x1024 and aligned to the "JRC2018U" reference brain template[82] using CMTK software in Fiji (for more details, see Flywire self-guided training). The aligned images were used to create a skeleton of the SELK neurons using the Single Neurite Tracer (SNT) plugin in Fiji (for more details, see Flywire self-guided training), which was then saved in *.swc* format. Only the most labeled trace of the SELK neuron (including the soma and main axon) was included in the skeleton to avoid false positive tracings. Finally, the SELK neuron skeletons were aligned to the FlyWire dataset[78] using the Flywire Gateway tool, taking the JRC2018U reference brain[82] as a template. The resulting point cloud in the FAFB of the FlyWire Sandbox was used to guide a search for nearby neurons to match the possible SELK neuron candidates' IDs previously identified.

Behavior

Proboscis Extension Reflex(PER)

PER to labellar stimulation was assessed following a standard protocol[84]. Flies were anesthetized on ice and individually immobilized on P200 tips, whose narrow end was cut so that only the fly's head could protrude from the opening, leaving the rest of the body, including legs, constrained inside the tip. After flies were recovered in a humidified chamber for 20 minutes, flies were water-satiated before testing *ad libitum*, discarding those that, after 5 minutes, continued extending their proboscis in response to water. Tastants were delivered

using a small piece of paper (Kimberly-Clark Kimtech, ref. 7552) and touching very gently the labellum for 2 seconds maximum, leaving a gap of 1 minute between stimulations. sucrose (Sigma Aldrich, ref. 102174662) and caffeine (Sigma-Aldrich, ref. 102143502) were diluted in miliQ sterile water appropriately. PER was manually recorded: only full proboscis extensions were counted as PER and registered as 1, considering partial or absent proboscis extension as 0. Finally, flies were tested at the end of the experiment with water as the negative control and 1 M of sucrose as the positive control. Only flies that showed negative PER for water and positive PER for 1 M of sucrose were included in the analysis.

flyPAD two choice assay

flyPAD assays were performed to study the feeding microstructure in a two-choice feeding paradigm as described previously[56], and several feeding parameters were measured individually in a high throughput manner. Individual flies were placed in individual arenas with two different food sources in independent well electrodes. The flyPAD hardware used comprised 56 individual chambers divided into two independent pieces of hardware, each consisting of 28 chambers connected to an independent computer. All tastants used were solved in water 1% low melting agarose (Lonza, ref. 50100). To transfer files to each chamber, flies were anesthetized in ice for 5 minutes and individually placed in the arena by mouth aspiration according to its sex and genotype. All the experiments began once all flies woke up and were active. Flies were allowed to feed at 25ºC for 60 minutes. After time ended, dead flies were annotated. flyPAD data were acquired using the Bonsai framework, and analyzed in MATLAB using custom-written software delivered by *Itskov et al., 2014*[56]. Then, specific *R* software scripts developed by the lab were applied to analyze the bulk of flyPAD experiment data. Only those flies that performed more than 2 bouts and 25 sips were included in the analysis.

Statistical analysis

The sample size was determined based on preliminary experiments. Data were analyzed using *R* software v4.1.0 (R Foundation for Statistical Computing, Vienna, Austria, 2005; https://www.r-project.org) (code available upon request) and plotted using *R* or *Graphpad Prisms 6*. The statistical test is determined in the figure legend for each of the plots. The Bonferroni method was used when p-value correction for multiple comparisons was required. Except for PER and flyPAD experiments, quantitative data show their distribution by superimposing a boxplot. For the boxplots the whiskers are calculated as follows: the upper whisker equals the third quartile plus 1.5× the interquartile range (IQR) and the lower whisker equals the first quartile minus 1.5× the IQR. Any data points above the superior or below the

inferior whisker values are considered outliers. The outliers were included in the statistical comparisons as we performed non-parametric rank tests.

For PER experiments, data were analyzed using a generalized linear model based on a logistic regression set to a binomial distribution model (function glm () in *R* software), where the response of the flies is dependent of their genotype responding to different stimuli of sucrose and caffeine (glm() equation used below). Error bars represent the standard error of the proportion ($\sqrt{\mathrm{p}(1-\mathrm{p})/\mathrm{n}}$).

glm(Response ~ Genotype * Stimulus, data = PERdata, family = binomial)

For flyPAD experiments, a set of *R* software scrips developed by the lab was used to analyze the feeding microstructure behavior, which employs different statistical tests depending on the final goal of the analysis. The preference index is calculated as follows:

$$\text{Preference Index (PI)} = \frac{N_A - N_B}{N_{TOTAL}}$$

Bibliography

1. Chu, B., Chui, V., Mann, K. & Gordon, M. D. Presynaptic Gain Control Drives Sweet and Bitter Taste Integration in Drosophila. *Curr Biol* **24**, 1978–1984 (2014).

2. Inagaki, H. K., Panse, K. M. & Anderson, D. J. Independent, Reciprocal Neuromodulatory Control of Sweet and Bitter Taste Sensitivity during Starvation in Drosophila. *Neuron* **84**, 806–820 (2014).

3. LeDue, E. E. *et al.* Starvation-Induced Depotentiation of Bitter Taste in Drosophila. *Curr Biol* **26**, 2854–2861 (2016).

4. Yarmolinsky, D. A. *et al.* Coding and Plasticity in the Mammalian Thermosensory System. *Neuron* **92**, 1079–1092 (2016).

5. Vosshall, L. B. & Stocker, R. F. Molecular Architecture of Smell and Taste in Drosophila. *Annu Rev Neurosci* **30**, 505–533 (2007).

6. Montell, C. Drosophila sensory receptors—a set of molecular Swiss Army Knives. *Genetics* **217**, 1–34 (2021).

7. Dahanukar, A., Lei, Y.-T., Kwon, J. Y. & Carlson, J. R. Two Gr Genes Underlie Sugar Reception in Drosophila. *Neuron* **56**, 503–516 (2007).

8. Fujii, S. *et al.* Drosophila Sugar Receptors in Sweet Taste Perception, Olfaction, and Internal Nutrient Sensing. *Curr Biol* **25**, 621–627 (2015).

9. Dunipace, L., Meister, S., McNealy, C. & Amrein, H. Spatially restricted expression of candidate taste receptors in the Drosophila gustatory system. *Curr. Biol.* **11**, 822–835 (2001).

10. Wang, Z., Singhvi, A., Kong, P. & Scott, K. Taste Representations in the Drosophila Brain. *Cell* **117**, 981–991 (2004).

11. Scott, K. Gustatory Processing in Drosophila melanogaster. *Annu Rev Entomol* **63**, 15–30 (2018).
12. Thorne, N., Chromey, C., Bray, S. & Amrein, H. Taste Perception and Coding in Drosophila. *Curr. Biol.* **14**, 1065–1079 (2004).
13. Jenett, A. *et al.* A GAL4-Driver Line Resource for Drosophila Neurobiology. *Cell Reports* **2**, 991–1001 (2012).
14. Dionne, H., Hibbard, K. L., Cavallaro, A., Kao, J.-C. & Rubin, G. M. Genetic Reagents for Making Split-GAL4 Lines in Drosophila. *Genetics* **209**, 31–35 (2018).
15. Meissner, G. W. *et al.* A searchable image resource of Drosophila GAL4 driver expression patterns with single neuron resolution. *eLife* **12**, e80660 (2023).
16. Flood, T. F. *et al.* A single pair of interneurons commands the Drosophila feeding motor program. *Nature* **499**, 83–87 (2013).
17. Kain, P. & Dahanukar, A. Secondary Taste Neurons that Convey Sweet Taste and Starvation in the Drosophila Brain. *Neuron* **85**, 819–832 (2015).
18. Miyazaki, T., Lin, T.-Y., Ito, K., Lee, C.-H. & Stopfer, M. A gustatory second-order neuron that connects sucrose-sensitive primary neurons and a distinct region of the gnathal ganglion in the Drosophila brain. *J. Neurogenet.* **29**, 144–155 (2015).
19. Yapici, N., Cohn, R., Schusterreiter, C., Ruta, V. & Vosshall, L. B. A Taste Circuit that Regulates Ingestion by Integrating Food and Hunger Signals. *Cell* **165**, 715–729 (2016).
20. Kim, H., Kirkhart, C. & Scott, K. Long-range projection neurons in the taste circuit of Drosophila. *eLife* **6**, e23386 (2017).
21. Schwarz, O. *et al.* Motor control of Drosophila feeding behavior. *Elife* **6**, e19892 (2017).
22. Bohra, A. A., Kallman, B. R., Reichert, H. & VijayRaghavan, K. Identification of a Single Pair of Interneurons for Bitter Taste Processing in the Drosophila Brain. *Curr. Biol.* **28**, 847-858.e3 (2018).
23. Sterne, G. R., Otsuna, H., Dickson, B. J. & Scott, K. Classification and genetic targeting of cell types in the primary taste and premotor center of the adult Drosophila brain. *Elife* **10**, e71679 (2021).
24. Engert, S., Sterne, G. R., Bock, D. D. & Scott, K. Drosophila gustatory projections are segregated by taste modality and connectivity. *Elife* **11**, e78110 (2022).
25. Talay, M. *et al.* Transsynaptic Mapping of Second-Order Taste Neurons in Flies by trans-Tango. *Neuron* **96**, 783-795.e4 (2017).
26. Weiss, L. A., Dahanukar, A., Kwon, J. Y., Banerjee, D. & Carlson, J. R. The Molecular and Cellular Basis of Bitter Taste in Drosophila. *Neuron* **69**, 258–272 (2011).
27. Root, C. M., Ko, K. I., Jafari, A. & Wang, J. W. Presynaptic Facilitation by Neuropeptide Signaling Mediates Odor-Driven Food Search. *Cell* **145**, 133–144 (2011).

28. Krashes, M. J. *et al.* A Neural Circuit Mechanism Integrating Motivational State with Memory Expression in Drosophila. *Cell* **139**, 416–427 (2009).
29. Riemensperger, T. *et al.* Behavioral consequences of dopamine deficiency in the Drosophila central nervous system. *Proc. Natl. Acad. Sci.* **108**, 834–839 (2011).
30. Nässel, D. R. & Zandawala, M. Recent advances in neuropeptide signaling in Drosophila, from genes to physiology and behavior. *Prog Neurobiol* **179**, 101607 (2019).
31. Farhan, A. *et al.* The CCHamide 1 receptor modulates sensory perception and olfactory behavior in starved Drosophila. *Sci Rep-uk* **3**, 2765 (2013).
32. Inagaki, H. K. *et al.* Visualizing Neuromodulation In Vivo: TANGO-Mapping of Dopamine Signaling Reveals Appetite Control of Sugar Sensing. *Cell* **148**, 583–595 (2012).
33. Jaeger, A. H. *et al.* A complex peripheral code for salt taste in Drosophila. *Elife* **7**, e37167 (2018).
34. Lee, K.-S., You, K.-H., Choo, J.-K., Han, Y.-M. & Yu, K. Drosophila Short Neuropeptide F Regulates Food Intake and Body Size*. *J. Biol. Chem.* **279**, 50781–50789 (2004).
35. Wu, Q. *et al.* Developmental Control of Foraging and Social Behavior by the Drosophila Neuropeptide Y-like System. *Neuron* **39**, 147–161 (2003).
36. Yoshinari, Y. *et al.* The sugar-responsive enteroendocrine neuropeptide F regulates lipid metabolism through glucagon-like and insulin-like hormones in Drosophila melanogaster. *Nat. Commun.* **12**, 4818 (2021).
37. Cannell, E. *et al.* The corticotropin-releasing factor-like diuretic hormone 44 (DH44) and kinin neuropeptides modulate desiccation and starvation tolerance in Drosophila melanogaster. *Peptides* **80**, 96–107 (2016).
38. Nässel, D. R. Leucokinin and Associated Neuropeptides Regulate Multiple Aspects of Physiology and Behavior in Drosophila. *Int J Mol Sci* **22**, 1940 (2021).
39. Haro, M. de *et al.* Detailed analysis of leucokinin-expressing neurons and their candidate functions in the Drosophila nervous system. *Cell Tissue Res.* **339**, 321–336 (2010).
40. Zandawala, M. *et al.* Modulation of Drosophila post-feeding physiology and behavior by the neuropeptide leucokinin. *Plos Genet* **14**, e1007767 (2018).
41. Al-Anzi, B. *et al.* The Leucokinin Pathway and Its Neurons Regulate Meal Size in Drosophila. *Curr Biol* **20**, 969–978 (2010).
42. Murakami, K. *et al.* translin Is Required for Metabolic Regulation of Sleep. *Curr. Biol.* **26**, 972–980 (2016).
43. Murphy, K. R. *et al.* Postprandial sleep mechanics in Drosophila. *Elife* **5**, e19334 (2016).
44. Yurgel, M. E. *et al.* A single pair of leucokinin neurons are modulated by feeding state and regulate sleep–metabolism interactions. *Plos Biol* **17**, e2006409 (2019).
45. Raji, J. I. & Potter, C. J. The number of neurons in Drosophila and mosquito brains. *Plos One* **16**, e0250381 (2021).

46. Asahina, K. *et al.* Tachykinin-Expressing Neurons Control Male-Specific Aggressive Arousal in Drosophila. *Cell* **156**, 221–235 (2014).
47. Feinberg, E. H. *et al.* GFP Reconstitution Across Synaptic Partners (GRASP) Defines Cell Contacts and Synapses in Living Nervous Systems. *Neuron* **57**, 353–363 (2008).
48. Thistle, R., Cameron, P., Ghorayshi, A., Dennison, L. & Scott, K. Contact Chemoreceptors Mediate Male-Male Repulsion and Male-Female Attraction during Drosophila Courtship. *Cell* **149**, 1140–1151 (2012).
49. Macpherson, L. J. *et al.* Dynamic labelling of neural connections in multiple colours by trans-synaptic fluorescence complementation. *Nat Commun* **6**, 10024 (2015).
50. Cachero, S. *et al.* BAcTrace, a tool for retrograde tracing of neuronal circuits in Drosophila. *Nat Methods* **17**, 1254–1261 (2020).
51. Zheng, Z. *et al.* A Complete Electron Microscopy Volume of the Brain of Adult Drosophila melanogaster. *Cell* **174**, 730-743.e22 (2018).
52. Gerhard, S., Lee, W.-C. A. & Wilson, R. The BrainCircuits.io platform. https://braincircuits.io/. (2023).
53. Sorkaç, A. *et al.* retro-Tango enables versatile retrograde circuit tracing in Drosophila. *eLife* **12**, e85041 (2023).
54. Sweeney, S. T., Broadie, K., Keane, J., Niemann, H. & O'Kane, C. J. Targeted expression of tetanus toxin light chain in Drosophila specifically eliminates synaptic transmission and causes behavioral defects. *Neuron* **14**, 341–351 (1995).
55. Clyne, J. D. & Miesenböck, G. Sex-Specific Control and Tuning of the Pattern Generator for Courtship Song in Drosophila. *Cell* **133**, 354–363 (2008).
56. Itskov, P. M. *et al.* Automated monitoring and quantitative analysis of feeding behaviour in Drosophila. *Nat Commun* **5**, 4560 (2014).
57. Snell, N. J. *et al.* Complex representation of taste quality by second-order gustatory neurons in Drosophila. *Curr Biol* **32**, 3758-3772.e4 (2022).
58. Kiral, F. R. *et al.* Brain connectivity inversely scales with developmental temperature in Drosophila. *Cell Reports* **37**, 110145 (2021).
59. Scaplen, K. M. *et al.* Transsynaptic mapping of Drosophila mushroom body output neurons. *Elife* **10**, e63379 (2021).
60. Ehrlich, A. *et al.* Tango-seq: overlaying transcriptomics on connectomics to identify neurons downstream of Drosophila clock neurons. *bioRxiv* 2024.05.22.595372 (2024) doi:10.1101/2024.05.22.595372.
61. Yarmolinsky, D. A., Zuker, C. S. & Ryba, N. J. P. Common Sense about Taste: From Mammals to Insects. *Cell* **139**, 234–244 (2009).
62. Barretto, R. P. J. *et al.* The neural representation of taste quality at the periphery. *Nature* **517**, 373–376 (2015).

63. Chen, X., Gabitto, M., Peng, Y., Ryba, N. J. P. & Zuker, C. S. A Gustotopic Map of Taste Qualities in the Mammalian Brain. *Science* **333**, 1262–1266 (2011).

64. Wang, L. *et al.* The coding of valence and identity in the mammalian taste system. *Nature* **558**, 127–131 (2018).

65. Harris, D. T., Kallman, B. R., Mullaney, B. C. & Scott, K. Representations of Taste Modality in the Drosophila Brain. *Neuron* **86**, 1449–1460 (2015).

66. Gordon, M. D. & Scott, K. Motor Control in a Drosophila Taste Circuit. *Neuron* **61**, 373–384 (2009).

67. Dobin, A. *et al.* STAR: ultrafast universal RNA-seq aligner. *Bioinformatics* **29**, 15–21 (2012).

68. Love, M. I., Huber, W. & Anders, S. Moderated estimation of fold change and dispersion for RNA-seq data with DESeq2. *Genome Biol.* **15**, 550 (2014).

69. Roberts, A., Trapnell, C., Donaghey, J., Rinn, J. L. & Pachter, L. Improving RNA-Seq expression estimates by correcting for fragment bias. *Genome Biol.* **12**, R22 (2011).

70. Gentleman, R. C. *et al.* Bioconductor: open software development for computational biology and bioinformatics. *Genome Biol.* **5**, R80 (2004).

71. Huber, W. *et al.* Orchestrating high-throughput genomic analysis with Bioconductor. *Nat. Methods* **12**, 115–121 (2015).

72. Hu, Y. *et al.* PANGEA: a new gene set enrichment tool for Drosophila and common research organisms. *Nucleic Acids Res.* **51**, W419–W426 (2023).

73. Ashburner, M. *et al.* Gene Ontology: tool for the unification of biology. *Nat. Genet.* **25**, 25–29 (2000).

74. Uchizono, S. *et al.* Deciphering the Genes for Taste Receptors for Fructose in Drosophila. *Mol Cells* **40**, 731–736 (2017).

75. Croset, V. *et al.* Ancient Protostome Origin of Chemosensory Ionotropic Glutamate Receptors and the Evolution of Insect Taste and Olfaction. *Plos Genet* **6**, e1001064 (2010).

76. Sánchez-Alcañiz, J. A., Zappia, G., Marion-Poll, F. & Benton, R. A mechanosensory receptor required for food texture detection in Drosophila. *Nat Commun* **8**, 14192 (2017).

77. Schindelin, J. *et al.* Fiji: an open-source platform for biological-image analysis. *Nat. Methods* **9**, 676–682 (2012).

78. Dorkenwald, S. *et al.* FlyWire: online community for whole-brain connectomics. *Nat Methods* **19**, 119–128 (2022).

79. Dorkenwald, S. *et al.* Neuronal wiring diagram of an adult brain. *Nature* **634**, 124–138 (2024).

80. Schlegel, P. *et al.* Whole-brain annotation and multi-connectome cell typing quantifies circuit stereotypy in Drosophila. *bioRxiv* 2023.06.27.546055 (2023) doi:10.1101/2023.06.27.546055.

81. Milyaev, N. *et al.* The Virtual Fly Brain browser and query interface. *Bioinformatics* **28**, 411–415 (2011).

82. Bogovic, J. A. *et al.* An unbiased template of the Drosophila brain and ventral nerve cord. *PLoS ONE* **15**, e0236495 (2020).

83. Costa, M., Manton, J. D., Ostrovsky, A. D., Prohaska, S. & Jefferis, G. S. X. E. NBLAST: Rapid, Sensitive Comparison of Neuronal Structure and Construction of Neuron Family Databases. *Neuron* **91**, 293–311 (2016).

84. Shiraiwa, T. & Carlson, J. R. Proboscis Extension Response (PER) Assay in Drosophila. *J Vis Exp* 193 (2007) doi:10.3791/193.